PERSPECTIVE

nature chemical biology

Cooperativity in macromolecular assembly

James R Williamson

The thermodynamic principle of cooperativity is used to drive the formation of specific macromolecular complexes during the assembly of a macromolecular machine. Understanding cooperativity provides insight into the mechanisms that govern assembly and disassembly of multicomponent complexes. Our understanding of assembly mechanisms is lagging considerably behind our understanding of the structure and function of these complexes. A significant challenge remains in tackling the thermodynamics and kinetics of the intermolecular interactions required for all cellular functions.

Formation of multicomponent macromolecular complexes is an essential feature of almost every aspect of cell function. Complex formation is governed by the chemical principles of kinetics and thermodynamics, although our quantitative understanding of many complexes is extremely limited. The field of systems biology continues to produce approximate inventories of components for complexes, and an approximate network of intermolecular interactions[1]. Structural biology continues to produce remarkable graphic images of complexes of ever-increasing size. However, a complete understanding of any macromolecular complex includes understanding its function, and the dynamics of its assembly and disassembly. This in turn requires a quantitative understanding of the thermodynamic and kinetic principles that govern macromolecular complex formation.

One important factor that is particularly relevant for assembly of macromolecular complexes is cooperativity, which helps drive complex formation. This Perspective is intended to serve as an introduction to the thermodynamics of assemblies for a broad audience interested in macromolecular assemblies. The general concept of cooperativity as it relates to macromolecular assembly is described, and several examples that illustrate emerging concepts are given.

Cooperativity

Cooperativity is a thermodynamic term that has taken on several different meanings in different contexts. Cooperativity is used to describe the complex interactions among identical ligands binding to multiple sites on an oligomeric protein, the classic example being oxygen binding to hemoglobin. Cooperativity is also used to describe the thermodynamics of macromolecular conformational transitions, such as protein folding or nucleic acid helix-coil transitions. Finally, the subject of the present review is a discussion of cooperativity observed in the thermodynamics of forming multicomponent complexes that are essential features of cellular biology.

The essential feature of all of these manifestations of cooperativity is thermodynamic linkage, which is a fancy way of saying that the binding between molecules is connected through the structures. For hemoglobin, the fourth and last oxygen molecule binds much more tightly than the first oxygen due to changes in the protein structure induced by the first ligands[2]. For protein folding, a stable hydrophobic core is constructed out of many weak interactions among the protein side chains arranged to pack tightly and exclude solvent[3]. For macromolecular assemblies, cooperativity ensures that the whole is more stable than the sum of its parts, which drives complex assembly.

Cooperativity in multicomponent complexes

The first step in any assembly process involves the formation of a binary complex from two individual components (A + B ⇔ AB, **Fig. 1a**). In general, complex formation is reversible, and the AB complex can dissociate into the two components, making this binding reaction a dynamic equilibrium. The relative amounts of free A and B, and AB complex, are determined by the balance of the rates of the association and disassociation reactions. The rates are dependent on two factors: the concentrations of the components, and the fundamental rate constants (k_{on}, k_{off}) that are a property of the binding reaction.

The assembly mechanism for macromolecular complexes can be broken down into such elementary steps, where each component of the complex is added in turn. The simplest case to consider for cooperative binding is a three-component system, where A and B can form an AB complex with equilibrium constant K_1, and where A and C can also form an AC complex with equilibrium constant K_2 (**Fig. 1a**). Cooperativity addresses how binding of B or C to the common partner A affects binding of the other. Do they help each other bind, do they hurt each other's binding or do they bind independently?

The thermodynamic construction that helps address this issue is known as a thermodynamic cycle[4,5] (**Fig. 1b**). The ternary ABC complex can be formed by two different possible routes, where B binds first, followed by C, or where C binds first, followed by B. Two additional equilibrium constants are shown (**Fig. 1b**), which are the binding of C to the preformed AB complex (K_3) and the binding of B to the preformed AC complex (K_4). The overall thermodynamics of forming the ABC complex from A cannot depend on the path taken around the cycle, and it must be true that $K_1K_3 = K_2K_4$. Equivalently, the free energies from both pathways must sum to the same amount, giving $\Delta G°_1 + \Delta G°_3 = \Delta G°_2 + \Delta G°_4$.

The two binding reactions that are represented horizontally in **Figure 1b** both involve binding of B to A, and the two binding reactions represented vertically both involve binding of C to A. The difference between the two horizontal and two vertical reactions is the presence or absence

James R. Williamson is in the Departments of Molecular Biology and Chemistry, and the Skaggs Institute for Chemical Biology, The Scripps Research Institute, 10550 North Torrey Pines Road, La Jolla, California 92037, USA.
e-mail: jrwill@scripps.edu

Published online 18 July 2008; doi:10.1038/nchembio.102

of the third component, and this difference corresponds to the coupling free energy for binding, $\Delta\Delta G$. The expression for $\Delta\Delta G$ can be obtained by subtraction of $\Delta G°_4$ from the left-hand side of the second equation in **Figure 1b**, and subtraction of $\Delta G°_3$ from the right-hand side, giving $\Delta\Delta G = \Delta G°_1 - \Delta G°_4 = \Delta G°_2 - \Delta G°_3$.

The significance of the coupling free energy $\Delta\Delta G$ is illustrated in **Figure 1c**, focusing on the difference in the two horizontal reactions involving binding of B. If binding of B is enhanced by the presence of C, then $\Delta G°_1 > \Delta G°_4$, and $\Delta\Delta G > 0$, and the binding of B and C have positive cooperativity. If binding of B is hindered by the presence of C, then $\Delta G°_1 < \Delta G°_4$, and $\Delta\Delta G < 0$, and the binding of B and C have negative cooperativity. If binding of B is unaffected by the presence of C, then $\Delta G°_1 = \Delta G°_4$, and $\Delta\Delta G = 0$, meaning the binding of the two ligands is independent. A completely equivalent set of statements can be made for vertical reactions of binding of C with respect to B in terms of $\Delta G°_2$ and $\Delta G°_3$.

Manifestations of cooperativity

There are many ways that the energetic gains for cooperative interactions can be realized, but they can be conceptualized in two ways (**Fig. 2a**,**b**). First, cooperativity can result from simple formation of mutually supporting interactions, as illustrated for formation of a ternary complex (**Fig. 2a**). Both B and C bind to adjacent sites on A, and upon formation of the ABC complex an additional interface between B and C is formed. For this example, the free energy of binding is taken to be proportional to the buried surface area between the components, resulting in a free energy of $\Delta G°_1 = -2$ kcal mol^{-1} and $\Delta G°_2 = -4$ kcal mol^{-1} for binding of B or C to A, respectively. Binding of the second component to form the ternary complex generates an additional kcal mol^{-1} of binding energy between B and C, so that $\Delta G°_3 = -6$ kcal mol^{-1} and $\Delta G°_4 = -4$ kcal mol^{-1}. The coupling free energy $\Delta\Delta G = 2$ kcal mol^{-1} can be clearly attributed to the simultaneous formation of intermolecular interactions at adjacent sites.

The second way that cooperativity can be manifested is a much more subtle effect of conformational changes that can occur upon binding (**Fig. 2b**). In this example, there is no direct contact between components B and C, but they are energetically coupled through two different conformations of their common partner A. In this illustrative model, one conformation of A is flat, while the other conformation has a knob and a hole that are complementary to a knob and a hole on B and C, respectively. In this example, it is assumed that there is a +1 kcal mol^{-1} penalty included to shift A from the flat to the knob and hole conformation, resulting in $\Delta G°_1 = -1$ kcal mol^{-1} and $\Delta G°_2 = -3$ kcal mol^{-1} for binding of B and C, respectively. After binding of the first ligand, A is now preorganized for binding of the second ligand, and the full binding interaction of each second ligand is realized as $\Delta G°_3 = -4$ kcal mol^{-1} and $\Delta G°_4 = -2$ kcal mol^{-1}. In this example, even though B and C do not interact directly, their binding is coupled through the structure of A by a conformational change, giving a positive free energy of coupling, $\Delta\Delta G = 1$ kcal mol^{-1}. These two instances are not mutually exclusive, and a range of combinations of formation of common interfaces accompanied by conformational changes can occur. In addition, coupling between binding reactions can be effected by changes in protonation, modification, ion binding or binding of other small ligands.

Assemblies as a network of interactions

The ternary complex (**Fig. 2a**) can be represented in a straightforward way using a thermodynamic cycle, but for more complex assemblies with larger numbers of components, such a representation becomes more difficult to visualize. In fact, formation of the ternary complex ABC (**Fig. 2a**) might also occur by binding of B and C to form a BC complex,

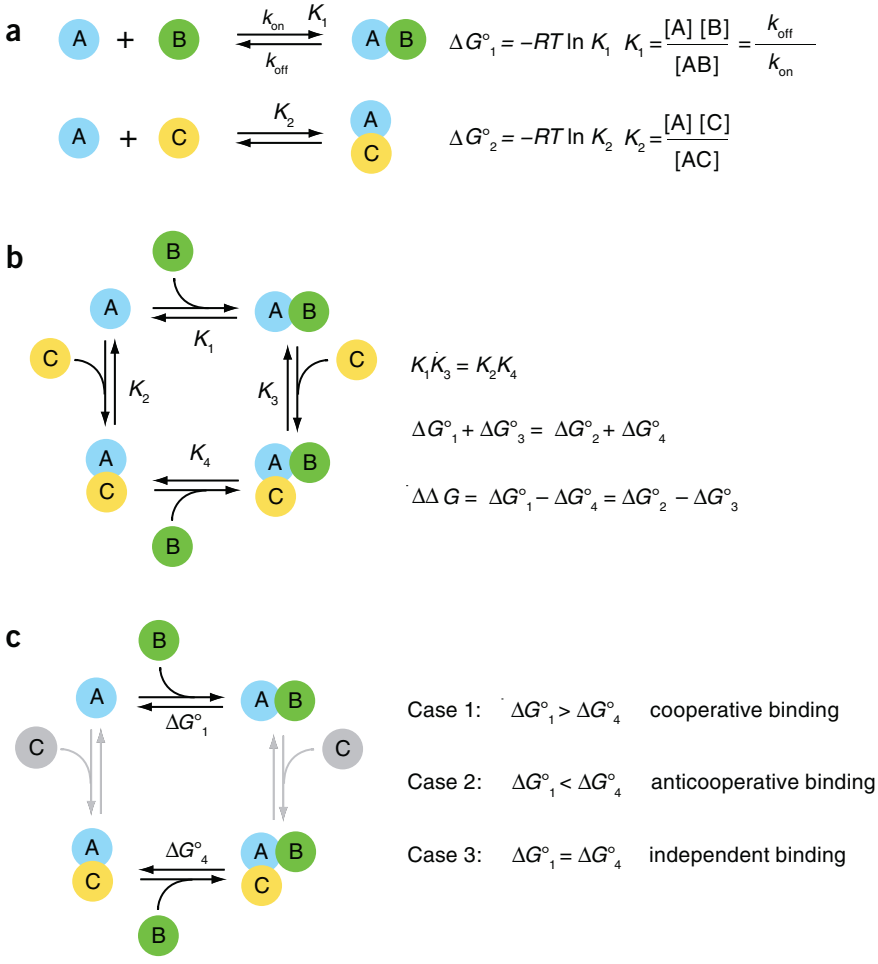

Figure 1 Thermodynamic cycles and cooperativity. (**a**) Hypothetical set of bimolecular complexes between component A and two other components (B and C), with the rate constants, equilibrium constants and free energies for complex formation. (**b**) A thermodynamic cycle for formation of the ternary complex ABC by two different possible routes: either B binds first, or C binds first. There are four equilibrium constants that describe the formation of the various complexes. Because they converge on the common product ABC, the thermodynamics must be independent of the pathway chosen around the cycle, and constraints are placed on the relative values of the equilibrium constants and hence the free energies. The thermodynamic coupling free energy ($\Delta\Delta G$) gives the difference between binding of one component in the presence of the other. (**c**) Definition of cooperativity in terms of binding of B in the presence or absence of C. The two vertical binding reactions are gray to emphasize the comparison of $\Delta G°_1$ and $\Delta G°_4$. If B binds better in the presence of C, the binding is cooperative. If B binds worse in the presence of C, the binding is anticooperative. In the third case, binding of B is independent of C, and there is no cooperativity.

followed by binding of A. The three possible pathways for forming a ternary complex are illustrated in **Figure 2c**, and it is possible to see the three interlocking thermodynamic cycles that describe the cooperativity in this system. The cycle shown in **Figure 2a** is the parallelogram formed by the blue and yellow arrows in **Figure 2c**, which are color-coded according to the protein binding reaction represented by each line in this graph. The second cycle is formed by the green and blue arrows, and the third is formed by the yellow and green arrows; together these three cycles form a thermodynamic cube[5], with one corner missing at the left.

Each vertex of the thermodynamic cube corresponds to one of the possible species in the reaction, which are the monomeric components, the three possible binary complexes, and the final ternary complex (the missing corner formally corresponds to the null state with no components). The connectivity among these complexes can be represented by a graph network (**Fig. 2d**), and the formation of the final ternary complex by sequential binding of monomers involves traversing the graph from left to right. Each path represents a possible mechanism for formation of the final complex. There are three mechanistically distinct pathways possible, each corresponding to the initial formation of three binary complexes. For larger assemblies, the number of possibilities increases factorially, and a network graph for formation of a heptameric complex is shown in **Figure 2e**, with the arrows omitted for clarity. This graph corresponds to a projection of a seven-dimensional thermodynamic hypercube into two dimensions, and the faces of this hypercube each correspond to a simple thermodynamic cycle that is characterized by a thermodynamic coupling energy between the binding of two of the seven components.

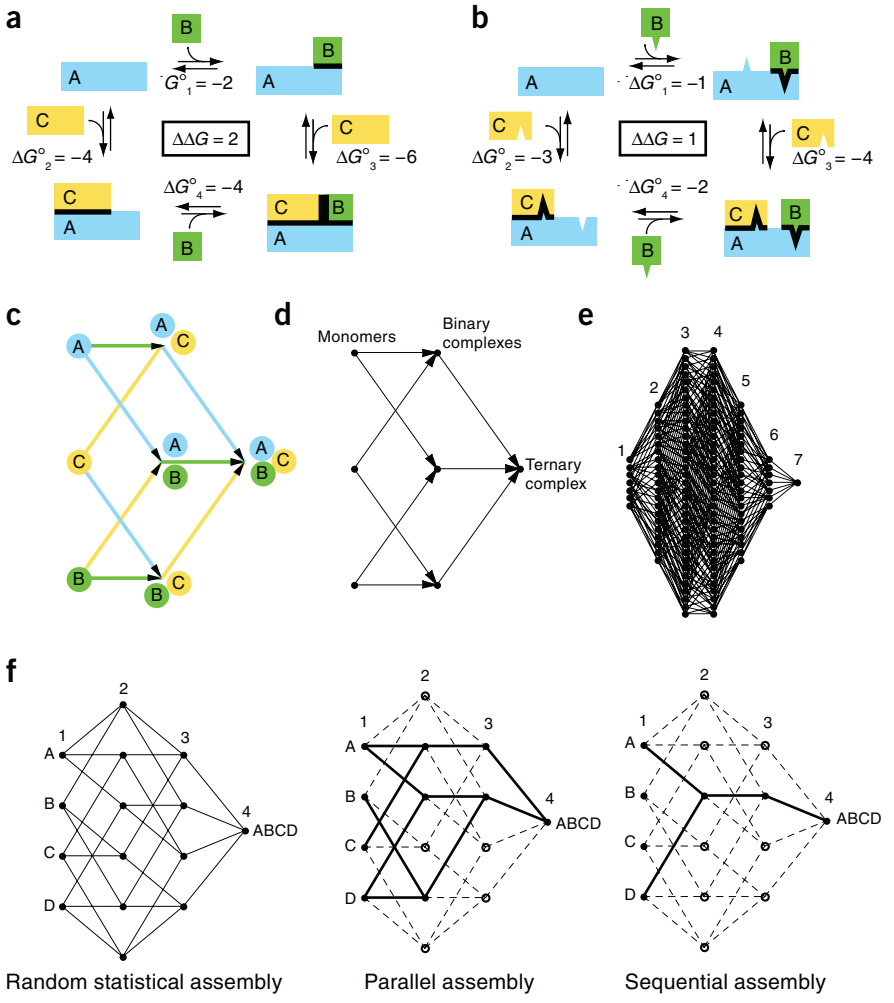

Figure 2 Mechanisms of cooperativity. (**a**) Hypothetical system illustrating cooperativity derived from mutually supporting molecular surfaces. The free energy of binding is assumed to be proportional to the buried surface area, indicated by the thick black line. (**b**) Hypothetical system illustrating cooperativity derived from induced fit. This example differs from that in **a** in that there is no direct contact between components B and C. The binding of the two is linked through a conformational change in the common partner A. In this example, there is a 1 kcal mol^{-1} penalty for changing the conformation of A, but the binding surfaces of AB and AC have the same values as in **a**. (**c**) Three interlocking thermodynamic cycles for formation of a ternary ABC complex forming the edges of a cube. (**d**) Graphical representation of the thermodynamic cube in **c**. Each vertex of the graph corresponds to one of the possible species, and each edge corresponds to a possible binding reaction. (**e**) Graphical representation of the seven-dimensional thermodynamic hypercube for formation of a heptameric complex, showing all possible sequential binding mechanisms. The numbers indicate the number of components in each of the species, or complexes. (**f**) Graphs of a four-dimensional thermodynamic hypercube for formation of a quaternary complex. The weight of all edges is equal, which indicates that all possible pathways can be used to assemble the complex, resulting in a statistical assembly process. If some species cannot be formed, there is a reduction in the number of pathways, resulting in a parallel pathway. An obligatory sequential assembly mechanism occurs when only one of the many possible pathways is traversed to form the complex.

The network graph for formation of a quaternary ABCD complex (**Fig. 2f**) illustrates three possible classes of mechanisms. If all possible sequential binding pathways among the four components can occur, the mechanism is a statistical assembly pathway with no preferred order for assembly, as indicated by the equal weight to all edges in the graphical representation (**Fig. 2d**). An intermediate mechanism involves parallel assembly by a subset of the possible pathways, where the absent pathways are represented by dashed edges and the species that are never observed are shown as open vertices. An obligatory sequential assembly mechanism involves traversing the graph using a defined set of edges.

Fully understanding an assembly mechanism involves identifying which species (vertices) are present, measuring the rates and free energies for each binding step (edges) and understanding the molecular structure of each complex. The three classes of mechanism (**Fig. 2f**) each have their advantages and disadvantages for ensuring efficient assembly. The statistical mechanism offers flexibility and does not require orchestration of a particular pathway, while the obligatory sequential mechanism requires complete orchestration of the series of steps (**Fig. 2f**). The orchestration of the assembly process can occur either through evolution of the intermolecular interfaces, or by recruitment of cofactors or chaperones (see below).

Physical models for assembly

Understanding how simple complexes with a few components form remains a challenge for biochemical and biophysical investigations. When the number of components increases,

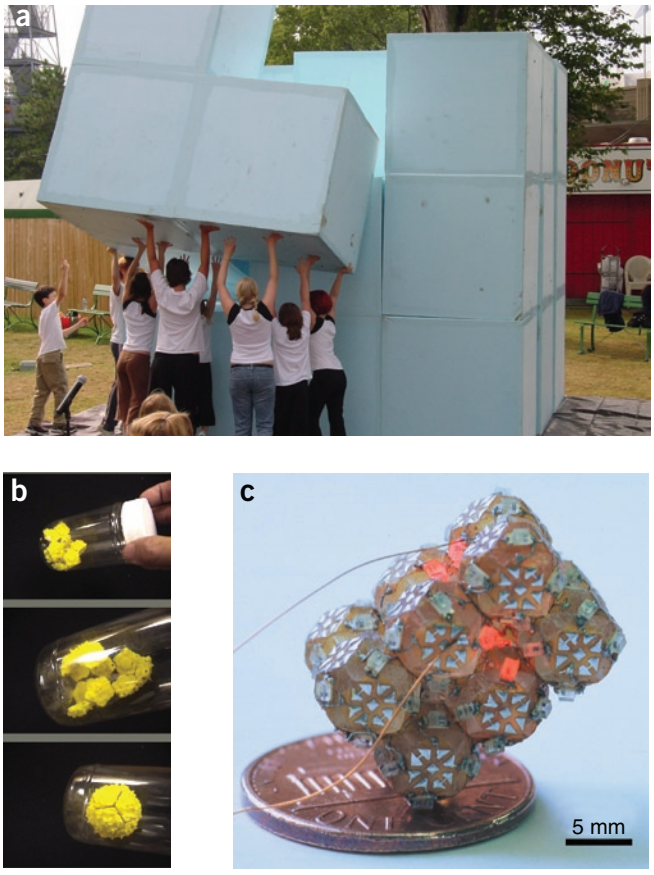

Figure 3 Physical models for assembly. (**a**) A large-scale model of Piet Hein's Soma cube puzzle (http://www.leonardosbasement.org/). In the symmetric cube assembly, shape complementarity is used to bury a large amount of exposed surface area, and there is a large cooperativity for assembling the final piece, in analogy to **Figure 2a**, as the hole in the puzzle precisely fits the incoming piece. This large-scale model also illustrates another common feature of complex assemblies: chaperones are often required to overcome large energetic barriers to a binding step. (**b**) An intriguing model for viral capsid assembly was developed in Art Olson's laboratory, where pentagonal capsid units are subjected to attractive energies supplied by small magnets embedded in the edges[6]. Twelve such units can be placed in a container, which is manually agitated to simulate diffusive molecular motions, and after a short period, partial assemblies of three or more capsid units are visible. With continued agitation, and some practice, a fully assembled dodecameric capsid results. (**c**) An electrical circuit assembled from polymer polyhedra that was developed in George Whiteside's laboratory[33]. The individual polyhedra were fabricated with wires and LEDs and a particular pattern of solder dots on their surface. Polyhedra with complementary patterns of dots 'bind' to each other in solution warmed over the melting temperature of the solder, and the resulting assemblies are frozen in place by cooling the solution. Again, shape complementarity and an attractive force result in formation of a defined structure. In this case the structure also forms a functional circuit with properties of fairly dubious electrical interest, but with profound implications for self-assembling systems.

as in the ribosome or a viral capsid, the challenge is fairly daunting (**Fig. 2e**). Analog physical models with reduced representation of the components can be used as tools to investigate the statistical properties of complex assembly mechanisms. Several existing physical models (**Fig. 3**) are analogs of the rigid assembly illustrated in **Figure 2a**, except with larger numbers of components.The assembly of the Soma cube (**Fig. 3a**; http://www.leonardosbasement.org/) involves formation of extensive complementary interfaces, yet there are many possible pathways to reach the final assembly. A simple model for virus capsid assembly provides a surprisingly rich set of insights into the nature and number of possible assembly intermediates[6] (**Fig. 3b**). Furthermore, the principles of self assembly have many other applications, including the nanofabrication of small-scale devices (**Fig. 3c**). All of these physical models for assembly embody one or more aspects of cooperativity and have the virtue that intermediates can be directly inspected to better understand the mechanism of assembly.

Cooperativity in Notch transcription factor complexes

Cooperative formation of multicomponent complexes provides a natural way to control assembly, and hence to control important processes in gene expression such as transcription, RNA processing and translation. Cooperative formation of DNA-protein complexes was first studied in the classic work on regulation of phage λ transcription by cI repressor protein binding to DNA[7,8]. Cooperative binding of transcriptional repressors and activators to DNA is likely to be the rule rather than the exception, but there are relatively few cases where detailed thermodynamic studies in combination with structural studies have been applied to this problem. One intriguing and recent example involves formation of a quaternary complex between DNA and three proteins (Notch-1, CSL and MAML) to regulate Notch signaling.

The Notch family of transmembrane receptors controls growth and development in a wide variety of cell types[9]. Binding of ligands to stimulate the Notch receptor results in intracellular cleavage of the receptor, liberating a soluble cytoplasmic signaling domain, or intracellular Notch (ICN)[10,11]. In the nucleus, Notch acts as an accessory transcription factor cooperatively with other factors to stimulate transcription of target genes. One partner of ICN is the multidomain protein CSL (CBF-1, suppressor of hairless, LAG-1), which binds directly to DNA, and a second partner is a coactivator protein from the MAML (mastermind-like) family[12]. In the absence of the ICN, CSL binds to DNA, but transcription is not activated, and binding of the ICN recruits the MAML coactivator to the CSL–DNA complex.

The crystal structure of the relevant domains of the Notch-1–CSL–MAML-1–DNA quaternary complex was solved in Steve Blacklow's laboratory (**Fig. 4a**)[13]. The DNA-protein interaction is mediated entirely through the CSL protein, and there are no DNA-protein contacts to the other two proteins. The MAML-1 coactivator forms an extended helix that makes extensive contacts with CSL at its C terminus, and with both CSL and the ankyrin repeat domain from Notch-1 (ANK) at its N terminus. This arrangement of the protein interfaces is very similar to the schematic complex shown in **Figure 2a**, where each protein contacts a composite surface formed by the other two.

In addition to solving the structure of this complex, Blacklow's laboratory also devised binding assays using fluorescence resonance energy transfer (FRET) to address the mechanism of formation of the activated quaternary complex[14]. The thermodynamic cycle for cooperative binding of the Notch-1 ANK domain and MAML-1 to CSL is shown in **Figure 4b**. The ANK domain (blue) binds only weakly to CSL (green) ($K_1 > 20\ \mu M$), and MAML-1 (red) alone does not bind detectably to CSL ($K_2 > 100\ \mu M$). However, the ANK domain binds well to CSL in the presence of MAML-1, with an overall apparent equilibrium constant $K_{app} \sim 0.6\ \mu M$, which is a composite of K_1 and K_3. From these measurements, a lower limit for the cooperativity can be calculated, and the presence of either protein increases the affinity of the other by at least 100-fold (**Fig. 4b**).

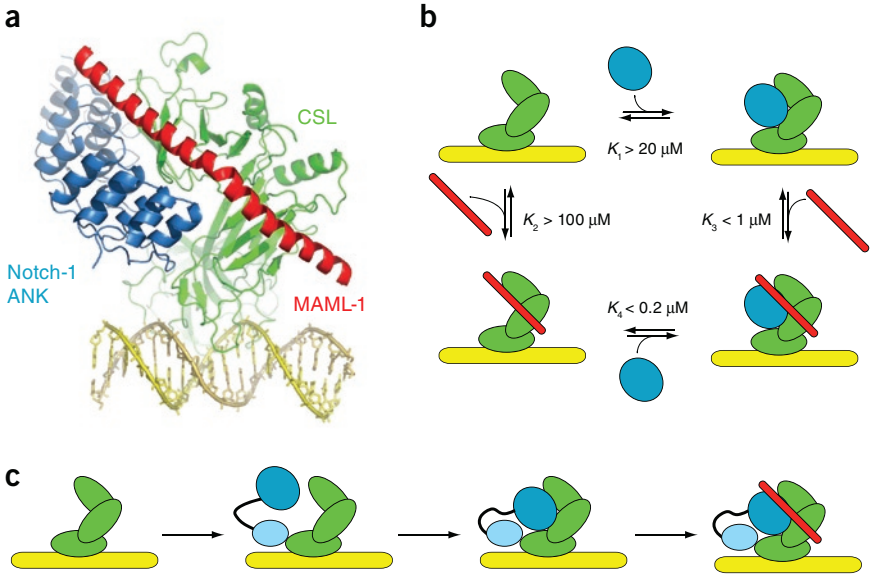

Figure 4 Cooperativity in Notch signaling. (**a**) Crystal structure of the Notch-1–CSL–MAML-1–DNA complex[13]. The ankyrin domain of Notch-1 (ANK) is shown in blue, CSL is shown in green, DNA is shown in yellow and MAML-1 is shown in red. (**b**) Thermodynamic cycle for formation of the quaternary complex, showing cooperativity measured for ANK and MAML-1 binding using a FRET assay. (**c**) The inferred mechanism of assembly of the activated Notch complex involves tight binding of another domain of Notch-1 (light blue), which tethers the ANK domain to the DNA without formation of a stable interface with CSL. Binding of MAML-1 is driven by formation of the extended surface of interaction with both ANK and CSL.

Despite the large interface between CSL and MAML-1, this interaction is weak in the absence of additional mutual interactions by the ANK domain of Notch-1. These thermodynamic measurements provide complementary insights into the nature of the coactivation of transcription to those obtained from the structure. These and other measurements allowed a mechanism for assembly of the activated complex to be constructed (**Fig. 4c**)[14]. Another Notch-1 domain (light blue, **Fig. 4c**) outside the ANK domain binds tightly to the DNA binding domain of CSL, but the ANK domain is not stably associated with CSL. Binding of MAML-1 co-stabilizes the ANK-CSL interaction to form the coactivated complex. Thus, the formation of the transcriptionally active Notch-1 complex requires the mutually supporting molecular interface that thermodynamically links Notch-1 and MAML-1 binding to the CSL–DNA complex. Either Notch-1 or MAML-1 alone is insufficient for activation, but cooperative binding of the two ensures that activation is only achieved in the presence of both protein signals.

Cooperativity in 30S ribosome assembly

The 30S ribosome is one of the most remarkable model systems for studying macromolecular assembly. The 30S ribosome is composed of a ~1,500-nucleotide 16S ribosomal RNA with 20 small associated proteins, but functional 30S subunits can be efficiently assembled from purified components *in vitro*. The thermodynamic assembly pathway was originally worked out by Nomura using an extensive set of order of addition experiments, where various subsets of proteins were tested for binding to 16S rRNA[15]. The information from these experiments is summarized in the now-classic Nomura assembly map (**Fig. 5a**). Each arrow in the Nomura map indicates a binding dependency, where proteins at the top bind directly to 16S rRNA while proteins below require prior binding of one or more proteins.

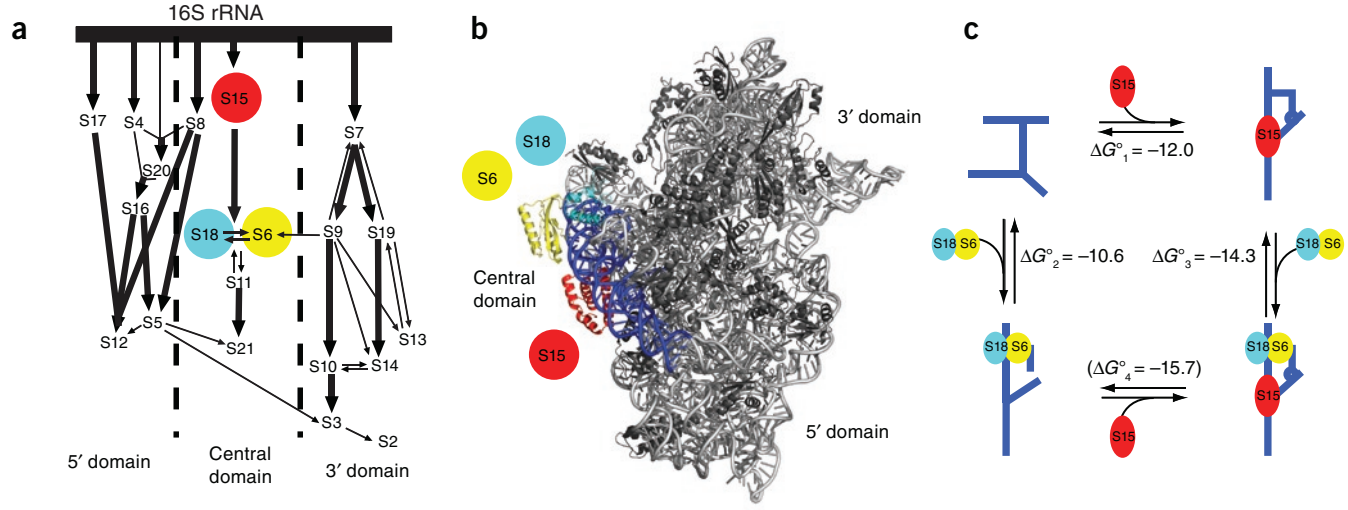

Figure 5 Cooperativity in 30S ribosome assembly. (**a**) The Nomura assembly map indicates protein binding dependencies for the 20 proteins in the 30S subunit. The central domain assembly cascade is initiated by binding of protein S15 (red), which is followed by binding of proteins S6 (yellow) and S18 (blue). (**b**) Ribbon diagram for the structure of the 30S ribosomal subunit with the location of the S15 (red), S6 (yellow) and S18 (blue) proteins. The minimal RNA binding fragment is shown in dark blue. (**c**) Thermodynamic cycle for formation of the S15–S6–S18–RNA complex. The free energies of binding for the various complexes are indicated, revealing that the cooperativity is 3.7 kcal mol^{-1}. Since there are no protein-protein interactions between S15 and the other two proteins, the cooperativity is manifested by folding of the RNA and stabilization of RNA tertiary structure.

The Nomura map is not a mechanism, but rather is a diagram that contains qualitative thermodynamic information about cooperativity. A particular cascade of protein binding dependencies is illustrated in **Figure 5a** for the central domain. Protein S15 (red) binds independently to 16S rRNA, but binding of proteins S6 (yellow) and S18 (blue) requires prior binding of S15. Furthermore, proteins S6 and S18 require each other for binding. The binding of these three proteins to 16S rRNA is therefore cooperative, but there is no information in the Nomura map about the energetics. Inspection of the crystal structure of the 30S ribosome (**Fig. 5b**)[16,17] provides some clues as to the nature of the cooperativity. Proteins S6 and S18 bind cooperatively because they form a heterodimer that binds as a unit to the RNA. However, there are no direct contacts between protein S15 and the S6–S18 dimer.

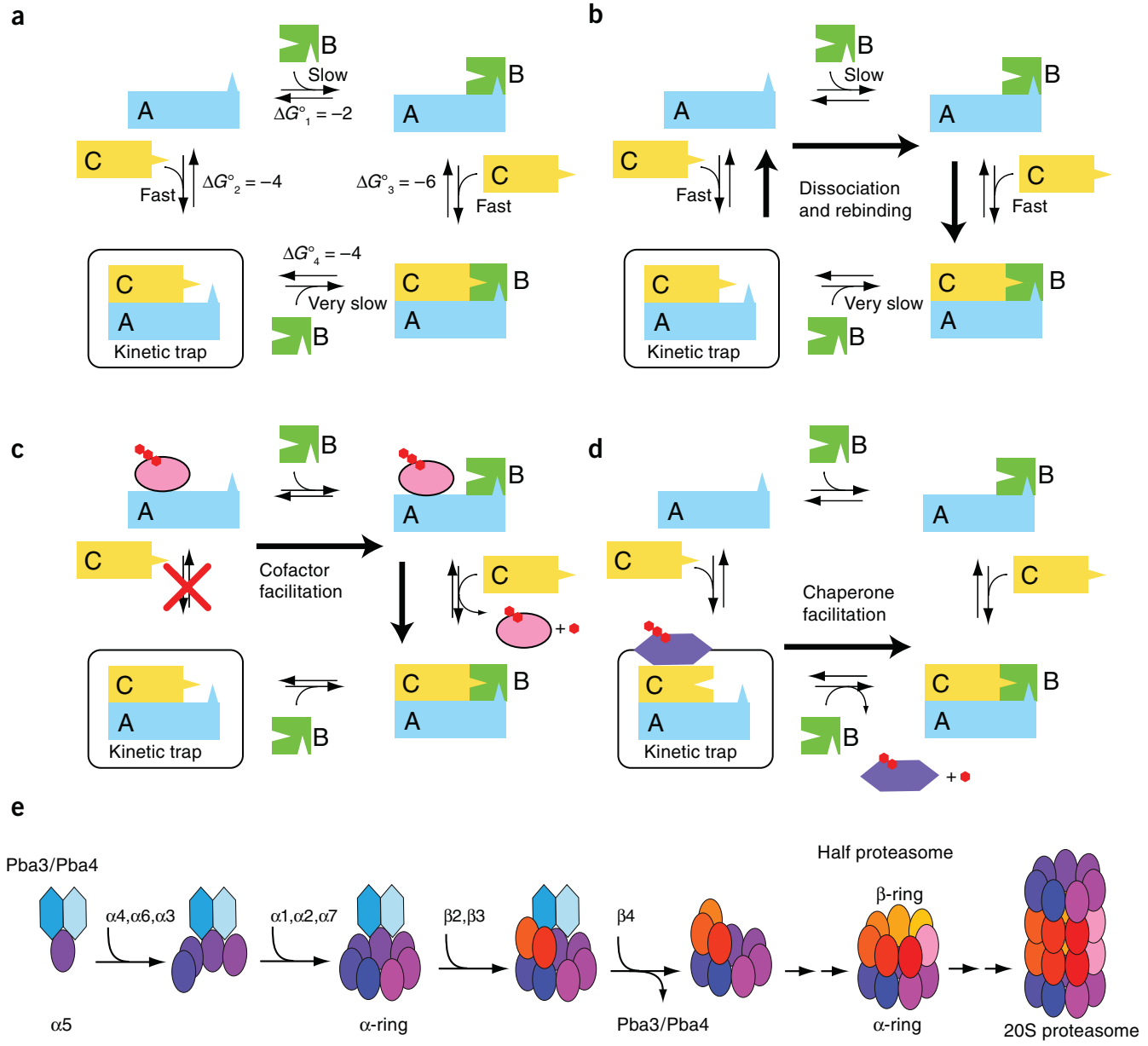

Figure 6 Kinetic traps, cofactors and chaperones. (**a**) A hypothetical model for formation of a kinetic trap. Formation of the ternary ABC complex can occur by binding of either B or C first. The system is contrived so that binding of B is slow, but that rapid formation of the AC complex results in a conformation where subsequent binding of B is difficult due to steric constraints. (**b**) Escape from the kinetic trap can be quite slow, since dissociation of the stable AC complex and subsequent productive binding of B is slow. (**c**) A cofactor (yellow) can participate in directing the assembly pathway by temporarily blocking the binding site for C, allowing the slow binding of B to occur. Dissociation of the cofactor might also be facilitated by a chemical reaction, such as nucleotide hydrolysis (red). (**d**) A chaperone (purple) can participate in the assembly by inducing a conformational change that allows the normally slow binding of B to occur. Function or release of the chaperone might also be facilitated by nucleotide hydrolysis (red). (**e**) The 20S proteasome is assembled in a series of steps from two heteroheptameric RNAs (far right). The assembly chaperone heterodimer complex Pba3/Pba4 binds selectively to the α5 monomer unit and stabilizes the binding of adjacent proteins, eventually resulting in formation of a heptameric α-ring. Assembly of the β-ring begins with the chaperone complex still bound, but upon binding of the β4 subunit the chaperone complex is released. Completion of the β-ring is followed by dimerization of two half-proteasomes to form the 20S complex. Several other chaperones participate in the assembly process (not shown).

In our laboratory, we have investigated the details of the cooperative binding of these three proteins, and the thermodynamic cycle for protein binding is shown in **Figure 5c**[18,19]. Proteins S15, S6 and S18 bind to a small RNA fragment derived from the central domain (blue, **Fig. 5a**,**b**). In the absence of S15, this RNA is not highly folded (**Fig. 5c**, upper right). Upon S15 binding, the RNA folds at two three-helix junctions, including formation of several RNA tertiary interactions. Binding of S15 folds the RNA and creates the binding site for the S6–S18 heterodimer.

Protein S15 binds to the RNA with high affinity (K_1 = 4 nM, $\Delta G°_1$ = –12.0 kcal mol^{-1}), and the heterodimer of S6–S18 binds more weakly (K_2 = 38 nM, $\Delta G°_2$ = –10.6 kcal mol^{-1}). There is strong cooperativity in binding among these proteins, for in the presence of S15, the heterodimer of S6–S18 binds very tightly (K_3 = 0.1 nM, $\Delta G°_3$ = –14.3 kcal mol^{-1}). The thermodynamic coupling energy is –3.7 kcal mol^{-1} (~380-fold), which represents the stabilization of the RNA tertiary structure by binding of S15 to create the binding site for S6 and S18. Each of the arrows in the Nomura map corresponds to thermodynamic linkage of protein binding with stabilization of RNA tertiary structure. The elements of parallel and sequential (cooperative) assembly ensure efficient folding and binding to form the complete 30S ribosome.

Assembly kinetics and escape from kinetic traps

The thermodynamic driving force for assembly ensures that the final complex is very stable, but the same factors that stabilize the final state also stabilize the intermediates on the assembly pathway. Kinetics can also play an important role in cooperative assembly, although kinetics are often more difficult to measure than thermodynamics, especially for complex systems. If problems occur during assembly by formation of an inappropriate or unfavorable structure, there is a danger that the problems become locked in by other stable native interactions, resulting in a kinetic trap where intermediates accumulate that can proceed only slowly or not at all on the assembly pathway.

As an example, a ternary ABC complex contrived to have a simple kinetic trap is illustrated (**Fig. 6a**). The thermodynamically favored pathway is binding of C to A, which is assumed to be fast. The alternative binding of B to A is assumed to be less favorable energetically and slower. In this example, the intermolecular interfaces between B and the other two molecules involve knob-into-hole interactions that create some steric restrictions. Formation of the AC complex results in close proximity of their respective knobs, making it very difficult to dock B because of a steric block. Thus, the more rapidly formed AC intermediate cannot proceed to formation of the ABC complex, making it a kinetic trap[20]. The only viable route to the ABC complex involves dissociation and rebinding (**Fig. 6b**). Each time the AC complex dissociates, there is some probability that B will bind first, followed by C binding, and eventually all proper ABC complexes will form by this very inefficient mechanism.

Kinetic traps in macromolecular complexes appear to be fairly common, and a variety of mechanisms have evolved to handle or avoid such kinetic traps. Assembly cofactors can bind to assembly intermediates to direct the assembly pathway (**Fig. 6c**,**d**). A cofactor can bind competitively with component C, allowing B to bind first. Dissociation of the cofactor is accompanied by binding of C to form the ternary complex. Assembly chaperones can bind directly to intermediates to induce conformational changes that permit the slow binding of B to occur, or to directly accelerate the binding of B. In addition, the binding of assembly cofactors or the activity of chaperones can be coupled to a chemical reaction, such as nucleotide hydrolysis or methylation.

Cooperativity and chaperones in proteasome assembly

Cofactors and chaperones can function in a variety of ways, including the facilitation of binding and dissociation. Helicases, GTPases, heat shock proteins and many other factors use binding and chemical reactions to control assembly, facilitate escape from kinetic traps or serve as checkpoints for the assembly process. Cofactors and chaperones have been implicated in many types of assemblies, but the structural and mechanistic basis for chaperone function has been elucidated for only a few systems. The proteasome is the assembly responsible for targeted protein degradation[21,22], and assembly of the eukaryotic proteasome involves chaperones at multiple stages to ensure efficient and proper assembly[23–29].

The eukaryotic proteasome core is composed of a dimer of two heteroheptameric rings, and there has been recent progress in understanding the functional role of chaperones in guiding proteasome assembly[23–28]. In particular, the earliest assembly steps are guided by a heterodimeric chaperone complex called Pba3/Pba4 in yeast[25,28] and Pac-1/Pac-2 in humans (**Fig. 6e**). The proteasome is composed of two α-rings with subunits α1–α7 and two β-rings with subunits β1–β7. Assembly of the α-ring is facilitated in part by binding of Pba3/Pba4 to the α5 subunit, which enhances the association of the adjacent α4 and α6 subunits. One of the observed functional roles for Pba3/Pba4 is to prevent misincorporation of an additional α4 subunit and to avoid stalling at the stage of incomplete α-rings[25]. After recruitment of the proper α3 subunit, the α-ring is completed and serves as a template for the initiation of β-ring assembly. After binding of the β2 and β3 subunits to the α-ring, binding of the β4 subunit is accompanied by release of the Pba3/Pba4 chaperone. Completion of the β-ring is followed by dimerization to complete the 20S proteasome (**Fig. 6e**).

Although the structures of the proteasome and some of the assembly intermediates have been determined, the thermodynamics and kinetics of the assembly process have not been quantitatively investigated to nearly the same extent as in these other example systems. Of course, thermodynamic studies require the availability of a suitable *in vitro* system using purified components. For this reason, the proteasome and other complex systems such as the eukaryotic ribosome remain significant challenges. Nevertheless, the underlying principles of cooperativity must be operative in formation of the proteasome. The challenge for assembling the proteasome lies in the accurate formation of the heteroheptameric rings from similar yet distinct intermolecular interfaces, and this challenge has been met in part by the evolution of assembly chaperones to populate one preferred mechanistic pathway that ensures proper assembly.

Summary

Mechanism is the third leg, along with structure and function, of the stool on which we sit for the understanding of biology. Any machine, for example an automobile, can be described in terms of its function (transportation) and its structure (four wheels, two doors, convertible, V8 engine). Truly understanding the mechanism by which the automobile carries out its function requires understanding how the thousands of parts are assembled and how they cooperate to turn a combustible fuel (octane—thermodynamics) into motion in a desired direction (miles per hour—kinetics).

As Tom Pollard sagely remarked, "Understanding mechanisms is genuinely difficult"[30]. His remarkable body of work on the assembly and disassembly of actin filaments underscores this statement, and underscores the need for annotating structure and function with kinetic and thermodynamic data that provide mechanistic insights. Networks of protein interactions inferred with systems biology and proteomic approaches reveal an extraordinary complexity of possibility. However, 'who interacts with who' is incomplete without 'when' and 'what for'. The basic tools of biophysics and biochemistry are in place to address these latter questions in terms of mechanistic understanding. An important

looming and remaining task is to adapt these techniques to facilitate rapid and parallel experimental assessment of the thermodynamics and kinetics of intermolecular interactions[31,32]. Only through such efforts will we attain an understanding of how the essential macromolecular machines of cellular function are assembled and how they work.

ACKNOWLEDGMENTS

The author thanks S. Edgcomb for helpful discussions and critical reading of the manuscript, S. Blacklow for critical comments and E. Vogel of Leonardo's Basement for the photo of the large Soma cube. This work was supported by a grant from the US National Institutes of Health (GM-53757 to J.R.W.).

Published online at http://www.nature.com/naturechemicalbiology/
Reprints and permissions information is available online at http://npg.nature.com/reprintsandpermissions/

1. Pawson, T. & Nash, P. Assembly of cell regulatory systems through protein interaction domains. *Science* **300**, 445–452 (2003).
2. Perutz, M.F., Wilkinson, A.J., Paoli, M. & Dodson, G.G. The stereochemical mechanism of the cooperative effects in hemoglobin revisited. *Annu. Rev. Biophys. Biomol. Struct.* **27**, 1–34 (1998).
3. Dill, K.A. *et al.* Principles of protein-folding—a perspective from simple exact models. *Protein Sci.* **4**, 561–602 (1995).
4. Horovitz, A. & Fersht, A.R. Strategy for analyzing the cooperativity of intramolecular interactions in peptides and proteins. *J. Mol. Biol.* **214**, 613–617 (1990).
5. Kranz, J.K. & Hall, K.B. RNA recognition by the human U1A protein is mediated by a network of local cooperative interactions that create the optimal binding surface. *J. Mol. Biol.* **285**, 215–231 (1999).
6. Olson, A.J., Hu, Y.H.E. & Keinan, E. Chemical mimicry of viral capsid self-assembly. *Proc. Natl. Acad. Sci. USA* **104**, 20731–20736 (2007).
7. Ackers, G.K., Johnson, A.D. & Shea, M.A. Quantitative model for gene-regulation by lambda-phage repressor. *Proc. Natl. Acad. Sci. USA* **79**, 1129–1133 (1982).
8. Johnson, A.D. *et al.* Lambda-repressor and cro—components of an efficient molecular switch. *Nature* **294**, 217–223 (1981).
9. Artavanis-Tsakonas, S., Rand, M.D. & Lake, R.J. Notch signaling: cell fate control and signal integration in development. *Science* **284**, 770–776 (1999).
10. Schroeter, E.H., Kisslinger, J.A. & Kopan, R. Notch-1 signalling requires ligand-induced proteolytic release of intracellular domain. *Nature* **393**, 382–386 (1998).
11. De Strooper, B. *et al.* A presenilin-1-dependent gamma-secretase-like protease mediates release of Notch intracellular domain. *Nature* **398**, 518–522 (1999).
12. Petcherski, A.G. & Kimble, J. LAG-3 is a putative transcriptional activator in the C-elegans Notch pathway. *Nature* **405**, 364–368 (2000).
13. Nam, Y., Sliz, P., Song, L.Y., Aster, J.C. & Blacklow, S.C. Structural basis for cooperativity in recruitment of MAML coactivators to Notch transcription complexes. *Cell* **124**, 973–983 (2006).
14. Del Bianco, C., Aster, J.C. & Blacklow, S.C. Mutational and energetic studies of notch1 transcription complexes. *J. Mol. Biol.* **376**, 131–140 (2008).
15. Held, W.A., Ballou, B., Mizushima, S. & Nomura, M. Assembly mapping of 30 S ribosomal proteins from *Escherichia coli*. Further studies. *J. Biol. Chem.* **249**, 3103–3111 (1974).
16. Schluenzen, F. *et al.* Structure of functionally activated small ribosomal subunit at 3.3 Å resolution. *Cell* **102**, 615–623 (2000).
17. Wimberly, B.T. *et al.* The structure of the 30S ribosomal subunit. *Nature* **407**, 327–339 (2000).
18. Recht, M.I. & Williamson, J.R. Central domain assembly: thermodynamics and kinetics of S6 and S18 binding to and S15-RNA complex. *J. Mol. Biol.* **313**, 35–48 (2001).
19. Recht, M.I. & Williamson, J.R. RNA tertiary structure and cooperative assembly of a large ribonucleoprotein complex. *J. Mol. Biol.* **344**, 395–407 (2004).
20. Dill, K.A., Fiebig, K.M. & Chan, H.S. Cooperativity in protein-folding kinetics. *Proc. Natl. Acad. Sci. USA* **90**, 1942–1946 (1993).
21. Hochstrasser, M. Ubiquitin-dependent protein degradation. *Annu. Rev. Genet.* **30**, 405–439 (1996).
22. Voges, D., Zwickl, P. & Baumeister, W. The 26S proteasome: a molecular machine designed for controlled proteolysis. *Annu. Rev. Biochem.* **68**, 1015–1068 (1999).
23. Hirano, Y. *et al.* Cooperation of multiple chaperones required for the assembly of mammalian 20S proteasomes. *Mol. Cell* **24**, 977–984 (2006).
24. Hirano, Y. *et al.* A heterodimeric complex that promotes the assembly of mammalian 20S proteasomes. *Nature* **437**, 1381–1385 (2005).
25. Kusmierczyk, A.R., Kunjappu, M.J., Funakoshi, M. & Hochstrasser, M. A multimeric assembly factor controls the formation of alternative 20S proteasomes. *Nat. Struct. Mol. Biol.* **15**, 237–244 (2008).
26. Le Tallec, B. *et al.* 20S proteasome assembly is orchestrated by two of chaperones in yeast distinct pairs and in mammals. *Mol. Cell* **27**, 660–674 (2007).
27. Li, X., Kusmierczyk, A.R., Wong, P., Emili, A. & Hochstrasser, M. β-subunit appendages promote 20S proteasome assembly by overcoming an Ump1-dependent checkpoint. *EMBO J.* **26**, 2339–2349 (2007).
28. Yashiroda, H. *et al.* Crystal structure of a chaperone complex that contributes to the assembly of yeast 20S proteasomes. *Nat. Struct. Mol. Biol.* **15**, 228–236 (2008).
29. Rosenzweig, R. & Glickman, M.H. Forging a proteasome alpha-ring with dedicated proteasome chaperones. *Nat. Struct. Mol. Biol.* **15**, 218–220 (2008).
30. Pollard, T.D. Regulation of actin filament assembly by Arp2/3 complex and formins. *Annu. Rev. Biophys. Biomol. Struct.* **36**, 451–477 (2007).
31. Torres, F.E. *et al.* Enthalpy arrays. *Proc. Natl. Acad. Sci. USA* **101**, 9517–9522 (2004).
32. Velazquez-Campoy, A. & Freire, E. ITC in the post-genomic era...? Priceless. *Biophys. Chem.* **115**, 115–124 (2005).
33. Gracias, D.H., Tien, J., Breen, T.L., Hsu, C. & Whitesides, G.M. Forming electrical networks in three dimensions by self-assembly. *Science* **289**, 1170–1172 (2000).